Forest Type Mapping using Object-specific Texture Measures from Multispectral Ikonos Imagery: Segmentation Quality and Image Classification Issues

Minho Kim, Marguerite Madden, and Timothy A. Warner

Abstract

This study investigated the use of a geographic object-based image analysis (GEOBIA) approach with the incorporation of object-specific grey-level co-occurrence matrix (GLCM) texture measures from a multispectral Ikonos image for delineation of deciduous, evergreen, and mixed forest types in Guilford Courthouse National Military Park, North Carolina. A series of automated segmentations was produced at a range of scales, each resulting in an associated range of number and size of objects (or segments). Prior to classification, the spatial autocorrelation of each segmentation was evaluated by calculating Moran's I using the average image digital numbers (DNs) per segment. An initial assumption was made that the optimal segmentation scales would have the lowest spatial autocorrelation, and conversely, that over- and under-segmentation would result in higher autocorrelation between segments. At these optimal segmentation scales, the automated segmentation was found to yield information comparable to manually interpreted stand-level forest maps in terms of the size and number of segments. A series of object-based classifications was carried out on the image at the entire range of segmentation scales. The results demonstrated that the scale of segmentation directly influenced the object-based forest type classification results. The accuracies were higher for classification of images identified from a spatial autocorrelation analysis to have an optimal segmentation, compared to those determined to have over- and under-segmentation. An overall accuracy of 79 percent with a Kappa of 0.65 was obtained at the optimal segmentation scale of 19. The addition of object-specific GLCM multiple texture analysis improved classification accuracies up to a value of 83 percent overall accuracy and a Kappa of 0.71 by reducing the confusion between evergreen and mixed forest types. Although some misclassification still remained because of local segmentation quality, a visual assessment of the texture-enhanced GEOBIA classification generally agreeable with manually interpreted forest types.

Minho Kim and Marguerite Madden are with the Center for Remote Sensing and Mapping Science (CRMS), Department of Geography, The University of Georgia, Athens, GA 30602 (mhkim73@uga.edu).

Timothy A. Warner is with the Department of Geology and Geography, West Virginia University, Morgantown, WV 26506.

Introduction

Natural resources managers have relied on the manual interpretation of aerial photographs since the 1940s and automated classification of medium resolution satellite image data since the 1970s (Colwell, 1960; Heller, 1975; Hoffer and Staff, 1975; Jensen, 1979; Lachowski *et al.*, 2000). Large-scale color infrared (CIR) aerial photographs have been manually interpreted to develop detailed forest databases and manage resources in state and federal conservation lands (Welch *et al.*, 1995; Lund *et al.*, 1997; Welch *et al.*, 1999). Manual interpretation to identify forest stands from aerial photographs is typically performed by human interpreters using basic image interpretation elements of tone, texture, shape, size, pattern, and associations (Avery, 1962; Teng *et al.*, 1997). Although this technique provides a high level of detail, it is a labor intensive classification of forest types from digital imagery (Welch *et al.*, 2002; Read *et al.*, 2003).

Very high spatial resolution (VHR) satellite imagery with spatial resolutions of similar magnitude to those of aerial photographs (1 to 4 m pixels) became available for resource inventory and monitoring with the successful launch of commercial imaging satellites in the late 1990s (Ehlers *et al.*, 2003; Ehlers, 2004). The VHR imagery is anticipated to be an alternative to aerial photos for characterization of forest structure and dynamics using automatic image classification techniques. In recent years, for example, Ikonos imagery has been frequently utilized for forest/vegetation mapping purpose using pixel-based image classification methods (Franklin *et al.*, 2001a; Asner and Warner, 2003; Read *et al.*, 2003; Wang *et al.*, 2004a; Wulder *et al.*, 2004; Metzler and Sader, 2005; Souza and Roberts, 2005). Pixel-based approaches, however, have limitations for use with VHR image classification because high spectral variability within classes decreases classification accuracy (Woodcock and Strahler, 1987; Marceau *et al.*, 1990; Shiewe *et al.*, 2001; Yu *et al.*, 2006; Lu and Weng, 2007). Pixel-based approaches also ignore the context and the spectral values of adjacent pixels (Fisher, 1997; Townshend *et al.*, 2000; Brandtberg and Warner, 2006). Various image classification techniques have

Photogrammetric Engineering & Remote Sensing
Vol. 75, No. 7, July 2009, pp. 819–829.

0099-1112/09/7507–0819/$3.00/0

been developed in remote sensing research, including object-based, textural, and contextual image classifications, in order to reduce the limitations associated with VHR images (Guo *et al.*, 2007; Lu and Weng, 2007). In this study, we employ an object-based image classification approach with the incorporation of texture for automatically interpreting forest types from VHR satellite imagery.

Geographic Object-based Image Analysis and Object-specific Texture

The geographic object-based image analysis (GEOBIA) approach has the potential to overcome inherent problems of high spectral variability within the same land-cover classes in VHR imagery (Yu *et al.*, 2006). The GEOBIA approach has been recognized as an important research area since the late 1990s, partly in the hope that this approach will emulate the human interpreters' ability to identify and delineate features of interest (Blaschke and Strobl, 2001; Schiewe *et al.*, 2001; Blaschke, 2003; Benz *et al.*, 2004; Meinel and Neubert, 2004).

Two steps typically involved in GEOBIA are: (a) image segmentation to produce image objects (or segments) that are the relatively homogeneous groups of pixels, and (b) image classification based on these image objects. The quality of segmentation is known to influence the accuracy of image classification (Dorren *et al.*, 2003; Meinel and Neubert, 2004; Addink *et al.*, 2007). Blaschke (2003) suggests estimation of the appropriate size of image objects (i.e., optimal segmentation scale) is a critical, but challenging, issue in GEOBIA. In addition, Dorren *et al.* (2003) and Ryherd and Woodcock (1996) emphasize the importance of image object size in forest mapping. However, there have been few studies to investigate the relationship between segmentation quality and forest type classification using VHR satellite imagery compared to a reliable reference data set. For example, with a manually interpreted and field verified data set for comparison, it is possible to examine how accurately object-based image classification can delineate the boundaries of forest types, and to investigate optimal segmentations for forest type mapping. Even though there have been a number of attempts to determine optimal segmentation (Wang *et al.*, 2004a; Kim and Madden, 2006; Feitosa *et al.*, 2006; Kim *et al.*, 2008), there are no specific guidelines on this issue and the selection procedure remains highly dependent on trial-and-error methods which subjectively influence segmentation quality (Definiens, 2004; Meinel and Neubert, 2004). For this reason, defining an optimal segmentation for the object-based classifications of various landscape units on the ground and developing methodologies for estimating the optimal segmentation can be regarded as urgent research issues. An example of a methodology to determine the appropriate segmentation for forest stands delineation is the spatial autocorrelation analysis employed by Kim *et al.* (2008). They performed a series of image segmentations and found three levels of segmentation in terms of spatial autocorrelation: over-segmentation, optimal segmentation, and under-segmentation. *Optimal segmentation* is considered a segmentation that produces desired image objects of the lowest autocorrelation in terms of spectral reflectance. On the contrary, *over- and under-segmentations* result in image objects of higher autocorrelation than optimal segmentation. Kim *et al.* (2008) computed and graphed Moran's I values across various segmentation scales to find these three levels of segmentation quality for forest stands.

In addition, the problem of within-class spectral variation of VHR imagery can potentially be addressed by a GEOBIA approach that uses a combination of spectral and texture information (Lu and Weng, 2007). The incorporation of texture in pixel-based classification approaches is a recurrent theme in remote sensing literature and has been successfully used to improve the accuracy of pixel-based forest/vegetation mapping with VHR satellite imagery (Zhang, 1999; Ferro and Warner, 2002). For example, Wang *et al.* (2004b) utilized first- and second-order texture measures to map mangrove species from VHR satellite images, such as Ikonos and QuickBird.

The grey-level co-occurrence matrix (GLCM) (Haralick *et al.*, 1973; Haralick and Shanmugam, 1974) is one of the most common algorithms for computing texture measures (Coburn and Roberts, 2004; Franklin *et al.*, 2000, 2001a, and 2001b; Zhang *et al.*, 2004). Common pixel-based texture is dependent on the size of the moving window (also called the kernel), specified by a particular number of columns and rows, used in the texture calculation. In GEOBIA, texture is essentially computed for non-overlapping irregularly-shaped "windows" that correspond to individual image objects (Benz *et al.*, 2004). We term such texture *object-specific texture* to distinguish it from texture computed with overlapping, moving kernels. When using kernel-based texture, it has been reported that between-class texture tends to degrade the overall performance of kernel-based texture classification (Ferro and Warner, 2002). However, between-class texture is potentially excluded by computing texture based only on pixels from within the boundary of an image object, as long as the quality of the segmentation is reliable. In addition, because image objects can potentially vary in size, object-specific texture is not inherently limited to a single scale to the extent that a single fixed-kernel size texture is limited. Hay *et al.* (1996) conducted a study utilizing object-specific texture measures which were computed within individual triangulated areas, the vertices of which were derived from the centers of tree crowns. Although they did not adopt an image segmentation procedure, their calculation of texture is similar to that of the object-specific texture adopted in this study, and they found forest stand classification could be improved by adding texture information computed from triangulated areas of tree crowns.

Research Objectives

The overall research objective was to investigate object-based classification with GLCM texture measures, using a case study of forest type mapping in the Eastern U.S., 4-meter multispectral Ikonos imagery, and a comparison with a reliable manually interpreted forest data set.

The overall research objective was addressed through three research questions:

1. Does segmentation quality, associated with segmentation scale, directly influence the classification results of forest types from VHR satellite imagery? If so, which segmentation is optimal for forest type mapping?
2. Can we determine optimal segmentation scale(s) prior to actual object-based forest type classification?
3. Will classification accuracies be improved by adding texture measures in object-based image classifications? If so, for what forest types?

The first question is closely associated with finding optimal segmentation of meaningful image objects for forest type classification related to shape, size, and placement. Although segmentation can be conducted across all possible scales, there is no guideline to determine what scale will produce optimal segmentation or to estimate the scale before actual image classification. In this study, a series of object-based forest type classifications was performed to: (a) examine the effect of segmentation quality on classification results, (b) evaluate optimal segmentation scales for forest type mapping, (c) confirm the validation of spatial autocorrelation analysis for estimating optimal segmentation, and (d) compare the effects of object-specific texture measures on forest type classification with a benchmark of a manually interpreted and field verified forest stands database. In addition, the boundary delineation of forest types from object-based classification was compared to the boundaries of a forest stands database derived from manual interpretation.

Study Area and Data

The study site is the National Park Service (NPS) Guilford Courthouse National Military Park (GUCO) which is located in Greensboro, North Carolina (Figure 1). The geographic coordinates of the site are 36°07′39″ − 36°08′11″ N, and 79°49′56″ − 79°50′58″ W. The National Military Park is about 1 km^2 in area, and it is located in a region experiencing rapid urban sprawl (Hiatt, 2003). This remaining green space is heavily used for recreation by the surrounding residents, placing increasing pressure on park managers to protect its natural and cultural resources. The park is managed to preserve the vegetation and landscape of the battlefield in a state as similar as possible to that of the time of the American Revolution.

The vegetation of the GUCO park was mapped by the University of Georgia (UGA) Center for Remote Sensing and Mapping Science (CRMS) in conjunction with NPS and NatureServe as a part of the United States Geological Survey (USGS)-NPS National Vegetation Mapping Program (Madden and Jordan, 2004; NPS, 2008). CIR aerial photographs, acquired on 20 October 2000, at 1:12 000 scale, were utilized for manual interpretation of vegetation based on the National Vegetation Classification System (NVCS) with 19 association (community)-level forest classes for the GUCO park. An independent field-based assessment performed by NatureServe, a non-profit conservation organization, indicated that the overall classification accuracy of the GUCO vegetation geodatabase was 83 percent, with a Kappa of 0.81 (NatureServe, 2007). In this study, we collapsed the 19 floristic forest associations into three physiognomic formations (Figure 2): deciduous broad-leaved forest (DF), evergreen needle-leaved forest (EF), and mixed evergreen-deciduous forest (MF). These classes approximate the upper L3-Formation Hierarchy Level of the Federal Geographic Data Committee (FGDC) National Vegetation Classification Standard Version 2 (Draft) and will hereafter be referred to as forest types (FGDC, 2007).

A multispectral Ikonos image with 8-bit radiometric resolution and 4-meter spatial resolution was used for object-based forest type classifications of the park. The Ikonos image was acquired on 06 July 2002 (see Figure 1) and rectified to a 1999 USGS digital orthophoto quarter quadrangle (DOQQ) with a root-mean-square-error of ± 4 m. The CRMS vegetation geodatabase was employed to obtain training data sets for individual forest types and samples for evaluating classification accuracy. The sample points were obtained by stratified random sampling method and verified using the DOQQ and CIR air photos.

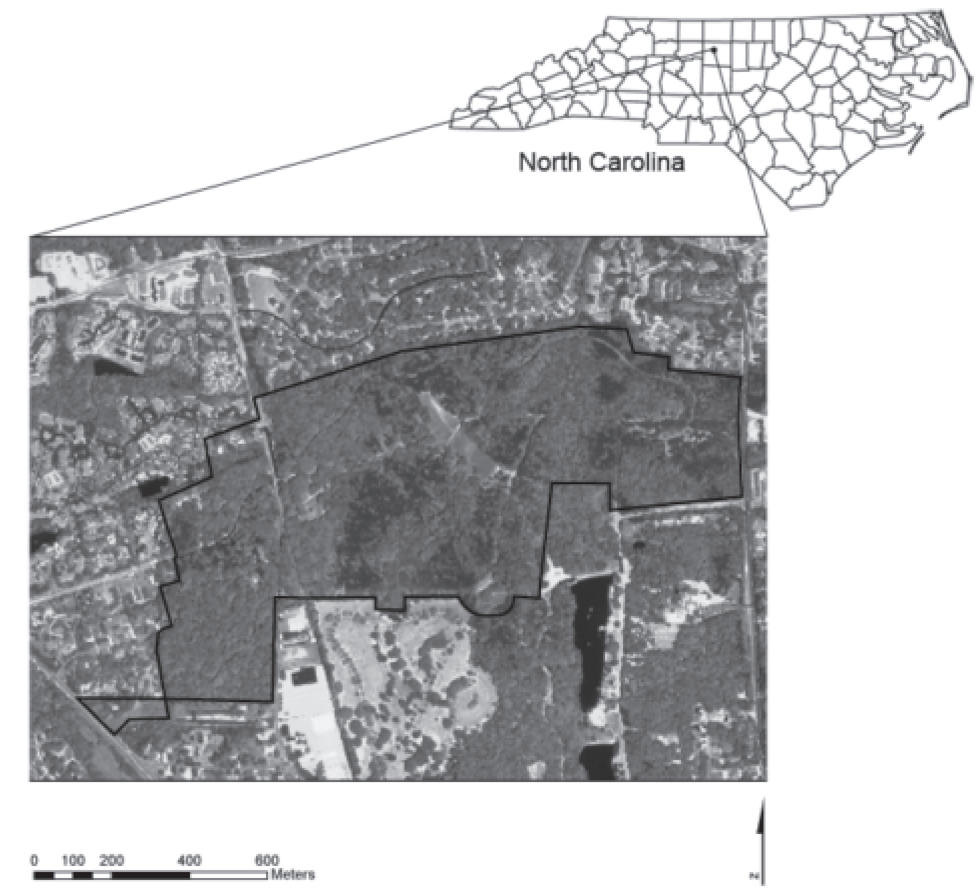

Figure 1. The Guilford Courthouse National Military Park study area depicted in a false color multispectral Ikonos image (bands 4, 3, and 2 as RGB). A color version of this figure is available at the ASPRS website: **www.asprs.org**.

Figure 2. Forest types of GUCO park from the CIR manual interpretation. A color version of this figure is available at the ASPRS website: **www.asprs.org**.

Methods

In order to compare the different GEOBIA classification strategies, a systematic series of classifications was undertaken. Before image segmentation and classification, we masked out non-forest areas such as pastures, home-sites, cemeteries and roads since the main concern of our study focused on forest types.

A series of segmentations was conducted using Definiens Developer, version 7.0 software. All spectral bands of the masked Ikonos image were used in the segmentations. Segmentations were produced using Definiens scale parameters (hereafter referred to as "scales") varying from 2 to 29, in steps of 1, producing a total of 28 segmentations. We chose 29 as a maximum scale because at this scale the largest image object was 45,920 m^2, which is similar to the maximum size of forest stands produced by the manual interpretation (46,286 m^2). The values of 0.1 and 0.9 were chosen for the ratios of shape and color, respectively. Each segmentation produced from the entire range of segmentation scales was separately processed using object-based forest type classification.

Spectral signatures of individual forest types were extracted from the four bands of the masked Ikonos image by using training data sets identified from the CRMS geodatabase, and then supervised object-based image classifications were performed by standard nearest neighbor classifier implemented in Definiens Developer. For these initial classifications, we utilized only the spectral values of the image to find the effect of segmentation quality and optimal segmentation for object-based forest type classification.

For the classifications involving object-specific texture classification, eight GLCM texture measures were employed: angular second moment (ASM), contrast (CON), correlation (COR), dissimilarity (DIS), entropy (ENT), homogeneity (HOM), mean (MEAN), and variance (VAR). The object-specific texture measures were computed using Definiens Developer from the near infrared (NIR) band of a segmentation which resulted in the highest overall classification accuracy when using spectral information alone. The NIR band was chosen for this segmentation because it contained the greatest range in spectral brightness values, and also carries important information for differentiating deciduous and coniferous species.

A directionally invariant texture measure was obtained by calculating the mean of the texture results in all four directions (0°, 45°, 90°, and 135°), which was then assigned to the associated image object. These object-specific texture measures were entered into forest type classifications as additional bands.

Accuracy Assessment

Based on the assumption that the manual map represented an optimal classification, overall accuracy and Kappa coefficient were employed to provide summary measures, and conditional Kappa coefficients to quantify accuracies of individual forest types based on agreement with the manual interpretation of forest types. A conditional Kappa coefficient indicates the classification accuracy of each individual class (Gong *et al.*, 1992), and it can be used to compare individual class differences between distinct classifications (Coburn and Roberts, 2004). In addition, error maps were generated to explore the spatial distribution of differences between the classifications. The CRMS forest type shapefile was rasterized with 4-meter pixel size and overlaid on the classified images in order to generate error maps which displayed the spatial distribution of differences between the automated GEOBIA classifications and the manual mapping, and to compute the percentages of classification confusions among three forest types.

Results and Discussion

Segmentation Quality for Forest Stands and Spatial Autocorrelation

Figure 3 illustrates a visual comparison of how the segmentation scale influences the quality of image segmentations. Figure 3a shows the manually-interpreted, community-level forest stands considered as the smallest unit on the GUCO park. Vegetation mapping for National Parks is normally carried out with a minimum mapping unit (MMU) of 0.5 ha (5,000 m^2), however for GUCO Park, a much smaller MMU was realized because photointerpreters included smaller mappable units of discernable forest communities. Thus, the smallest forest stand mapped was 240 m^2, with an average size of 4,025 m^2. The other parts of Figure 3 illustrate three levels of segmentation at four scales. The results at smaller segmentation scales were highly over-segmented, and the size of image objects was much smaller than the manually-interpreted forest stands, as shown in Figure 3b. As the scale increases, the segmentation results start to resemble the forest stands of the manual interpretation. In particular, the scales of 18 and 19 produced image segmentations most similar to the manually interpreted forest stands. Even at a scale of 18, the dashed-circle areas in Figure 3c indicate manually-interpreted forest stands that were divided into several image objects on the segmented image. Conversely, some forest stands on the manually-interpreted database corresponded to merged image objects as indicated by arrows in Figure 3c. The other segmentation at scale of 19 showed several image objects, produced with the scale of 18, were merged further and formed larger image objects illustrated by arrows in Figure 3d. Nevertheless, the segmentation from the scale of 19 was relatively similar to that of scale 18. At a scale of 26, the image was under-segmented, particularly in areas indicated by arrows (Figure 3e). These areas were composed of several image objects at scales of 18 and 19, but at the scale of 26, each area was represented as a single image object where more than two forest types were included.

In a previous evaluation of segmentation quality for GUCO park, Kim *et al.* (2008) found that optimal segmentations occurred at scales that were close to manually-interpreted

Figure 3. Over- and under-segmentation compared to manual interpretation: (a) manually-interpreted map, (b) over-segmentation at the scale of 4, (c) optimal segmentation at the scale of 18, (d) optimal segmentation at the scale of 19, and (e) under-segmentation at the scale of 26. A color version of this figure is available at the ASPRS website: **www.asprs.org**.

forest stands in terms of number and average size (Figure 4). The average sizes of image objects at the scales were 4,432 m^2 and 6,608 m^2, respectively. These object sizes are comparable to the average size of manually interpreted forest stands (4,025 m^2) indicating automatic segmentation can potentially delineate forest stands at least similar to that obtained from a manual interpretation.

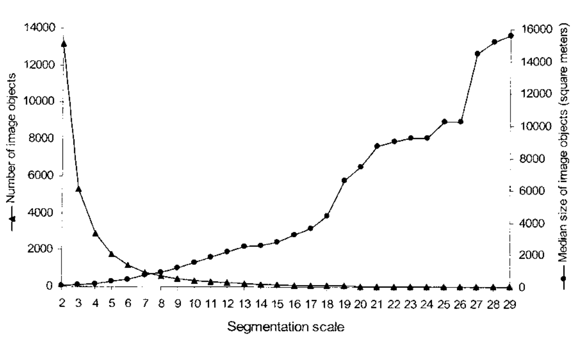

Figure 4. Median size and number of image objects produced at each segmentation scale.

In addition to image object size, quality of segmentation can be assessed by using spatial autocorrelation. Kim *et al.* (2008) assumed that with over-segmentation, as in Figure 3b, neighboring image objects would be spatially autocorrelated due to their similar mean spectral values. Similarly, the spatial autocorrelation of neighboring objects would be high with under-segmentation (as in Figure 3e) as the segments would tend to comprise mixtures of spectral values. On the other hand, they suggested that the least similarity in spectral values of adjacent segments would indicate optimal segmentation. Kim *et al.* (2008) found that over- and under-segmentations occurred when Moran's I index values were positive, while optimal segmentation was associated with lowest, even negative, index values (Figure 5).

Object-based Spectral Classification

The relationship between classification accuracy and segmentation scale is shown in Figure 6. Generally, the accuracy

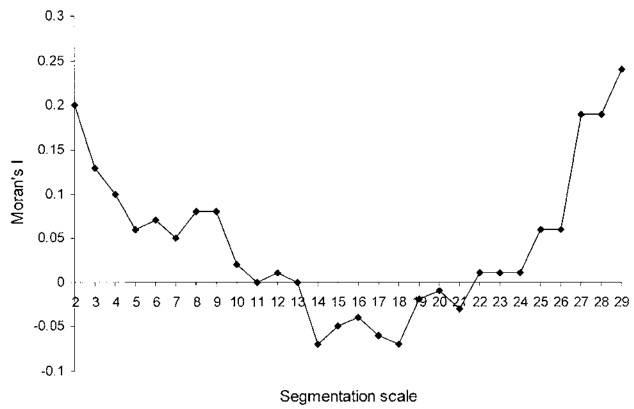

Figure 5. Moran's I graphed as a function of segmentation scale. (The figure was reprinted with permission of Springer Science and Business Media.)

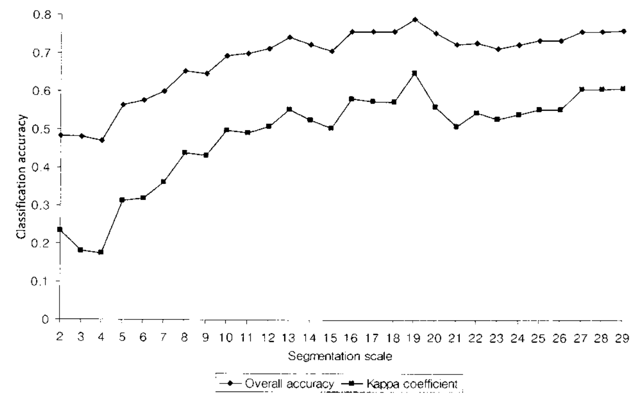

Figure 6. Object-based classification accuracies graphed against segmentation scales.

rises from the smallest scale of 2, with a peak accuracy at the scale of 19 (overall accuracy 79 percent and Kappa 0.65). By comparison, the scale of 18, which was determined to be the optimal scale based on image object size, has an overall accuracy of 76 percent with a Kappa of 0.57.

In general, Figure 6 shows lower overall classification accuracies for the scales that produced over- and under-segmentations, and higher accuracies for those that produced more optimal segmentations. The accuracies of forest type classification were directly influenced by the quality of segmentation related to the average size of image objects (see Figure 4). Higher classification accuracies were obtained at segmentations that resemble the average size of forest stands from the manual interpretation. This result supports our hypothesis that optimal segmentation scales for forest type mapping can create a meaningful segmentation that resembles stand-level forest polygons on manual interpretation, and the appropriate scale can be estimated by computing Moran's I values and graphing them against segmentation scales. As shown in Table 1, at the scale of 19, individual classification accuracies of deciduous forest based on spectral information alone were 85 percent and 90 percent for producer's and user's accuracies, respectively, with a Kappa of 0.76. However, the producer's accuracy of evergreen forest and the user's accuracy of mixed forest were 62 percent and 61 percent with Kappa of 0.64 and 0.52, respectively. Figure 7a shows a classification result that was derived at a scale of 19 with only spectral bands.

Table 1. Error Matrix of an Object-based Classification at the Scale of 19 using Spectral Bands

		Reference			
		DF	EF	MF	User's accuracy (%)
Classification	DF	144	13	3	90
	EF	11	46	6	73
	MF	15	15	47	61
Producer's accuracy (%)		85	62	84	

Overall accuracy: 79 %, Kappa coefficient: 0.65
DF Kappa coefficient: 0.76
EF Kappa coefficient: 0.64
MF Kappa coefficient: 0.52

In order to compare the edge boundaries and placement of image segments from the optimal scale of 19 versus manually-interpreted forest stands, the two data sets were overlaid to produce an "error" map as shown in Figure 7b. The classification error map depicts misclassifications visually and quantitatively between the automatic classification and the manual interpretation with differences generally being less than 10 percent. The percentage of misclassification between deciduous and evergreen forest types was 8 percent and that between deciduous and mixed forest was 6 percent when compared with manual interpretation. The confusion between evergreen and mixed forest types was 6 percent. The spectral information alone in object-based forest type classification produced higher confusion between pure and mixed forest types than between pure forest types. Therefore, object-specific texture classifications were adopted to reduce this classification confusion.

Object-specific Texture Classification

A total of eight object-specific GLCM texture measures were computed based on the segmentation that resulted in the best overall classification accuracies, i.e., at the scale of 19. Texture measures for the segmented objects were individually combined with the spectral bands of mean brightness values, and then entered into each object-based texture classification. Object-specific texture classification accuracy results using a single texture measure ranged from 60 percent (Kappa of 0.37) for GLCM homogeneity, to 79.3 percent (Kappa of 0.65) for GLCM mean (Figure 8). Compared to the 79 percent accuracy (Kappa of 0.65) of object-based classification using spectral bands alone, the addition of the GLCM mean texture measure enhanced overall accuracy by just 0.3 percent, and the incorporation of the remaining texture measures, except angular second moment and contrast, decreased classification accuracy.

As another way of using texture measures, the multiple texture analyses, which incorporated multiple texture measures simultaneously for object-specific texture classifications, were employed using the same segmentation scale (i.e., 19). Seven combinations of GLCM texture measures were investigated: all combinations of two, three, four, five, six, seven, and eight texture measures. Figure 9 illustrates the minimum, median, maximum, first quartile and third quartile of overall classification accuracies for texture combinations with two to

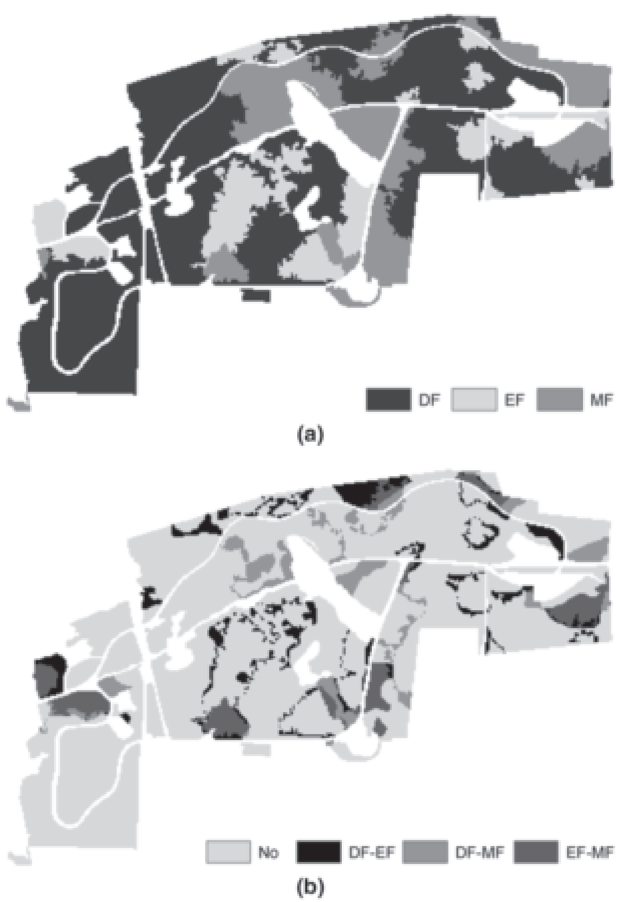

Figure 7. (a) Object-based classification of spectral data at a scale of 19, and (b) differences between the object-based classification and the manually interpreted map. A color version of this figure is available at the ASPRS website: **www.asprs.org**.

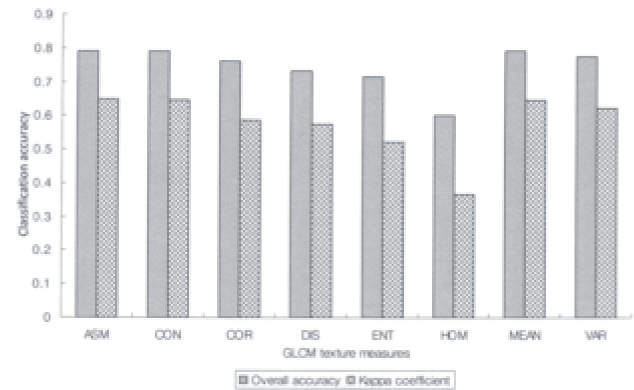

Figure 8. Classification accuracies using individual GLCM texture measures.

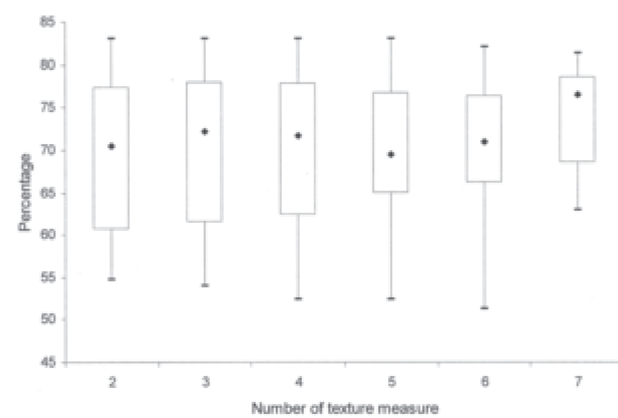

Figure 9. Box plot illustrating classification accuracies across possible combinations of GLCM texture measures. Each marker within individual boxes represents median values and the number on the abscissa represents the number of texture measures entered into classification.

seven measures. The incorporation of all eight texture measures resulted in an overall accuracy of 78 percent, with a Kappa of 0.64. The highest overall classification accuracies, with relatively uniform values of approximately 83 percent and Kappa values of 0.71, were obtained with selected combinations from two to five texture measures. For example, for just two texture measures, the combination that produced the highest accuracy was GLCM correlation and variance. The highest accuracy for three texture measures was obtained with GLCM correlation, variance, and dissimilarity. The highest accuracy for four texture measures was acquired with two different groups: GLCM contrast, correlation, dissimilarity, and variance; and GLCM correlation, dissimilarity, mean, and variance. The highest accuracy that was obtained with five texture measures was GLCM contrast, correlation, dissimilarity, mean and variance. A notable feature of this multiple texture analysis is that the incorporation of GLCM homogeneity texture measure generally degraded classification accuracies of the object-based texture classifications.

Besides these enhanced overall classification accuracies and Kappa coefficients using combined spectral and texture information, there also was notable improvement of individual classification accuracies for evergreen and mixed forest types. For example, as shown in Table 2, classification accuracies of evergreen and mixed forest types were generally improved

Table 2. Error Matrix of an Object-based Classification at the Scale of 19 using Spectral Bands and Texture Measures of GLCM Contrast, Correlation, Dissimilarity, and Variance

		Reference			
		DF	EF	MF	User's accuracy (%)
Classification	DF	145	13	7	88
	EF	10	58	3	82
	MF	15	3	46	72
Producer's accuracy (%)		85	78	82	

Overall accuracy: 83%, Kappa coefficient: 0.71
DF Kappa coefficient: 0.72
EF Kappa coefficient: 0.76
MF Kappa coefficient: 0.65

(ranging from 72 percent to 88 percent correct) by incorporating multiple texture measures in terms of producers' accuracy, user's accuracy and conditional Kappa coefficient. By adding GLCM contrast, correlation, dissimilarity and variance, the producer's and user's accuracies of evergreen forest type were improved by 16 percent and 9 percent, respectively, when compared with those accuracies from spectral information alone. In addition, the user's accuracy of mixed forest type was enhanced by 11 percent with four object-specific GLCM texture measures. Gains of 0.12 and 0.13 in conditional Kappa coefficients for evergreen and mixed forest types, respectively, were observed, although there was a slight decrease (i.e., 0.04) in the conditional Kappa coefficient of deciduous forest type. The other GLCM texture combinations, mentioned above, also enhanced classification accuracies by reducing the classification confusion between evergreen and mixed forest types. Overall, the accuracy of object-based classification could be improved through the incorporation of multiple GLCM texture measures, although not in all cases as shown in Figure 9 by the variation between the minimum and maximum accuracy achieved. Figure 10a illustrates a GEOBIA forest type classification result produced by using spectral information and GLCM texture measures of contrast, correlation, dissimilarity and variance.

This object-specific GLCM multiple texture analysis raises the question of why overall classification results were not enhanced beyond 83 percent. To answer this question, we produced a classification error map using an automatic classification result from a texture combination of GLCM contrast, correlation, dissimilarity and variance and the manually-interpreted forest stands, as shown in Figure 10b. In addition, we calculated the percentages of confused classification among the three forest types. The confusion percentages of DF-EF and DF-MF were the same as those from the spectral classification (i.e., 8 percent and 6 percent, respectively) even though the classification confusion between evergreen and mixed forest types was lowered to 2 percent. As illustrated in Figure 10b, the confusion between deciduous and evergreen forest types came from transition areas between the two types and local segmentation result that did not produce smaller evergreen stands designated by circles in Figure 10b. In addition, the confusion between deciduous and mixed forest types resulted from local segmentation quality even at the optimal scale of 19. The classification confusion between evergreen and mixed forest types also occurred because of local segmentation quality even after adding object-specific GLCM multiple texture measures. The confusion percentages and error map of this study revealed that the object-based forest type classification result could not perfectly resemble the manual interpretation possibly because of poor segmentation quality even at the optimal scale of 19 or due to the subjective nature of manual interpretation. At any rate, the quality of segmentation has a critical effect on forest type classifications when using object-based classification and VHR satellite imagery.

Overall, the object-based classification combined with object-specific GLCM texture produced a map of forest types that most closely resembled the manually interpreted forest type map (see Figure 10a). In addition, the best object-based classification could be converted to a vector polygon format representing forest type stands. This vector file of forest type stands can be used for further GIS analysis, e.g., vegetation modeling or forest fire fuels analysis.

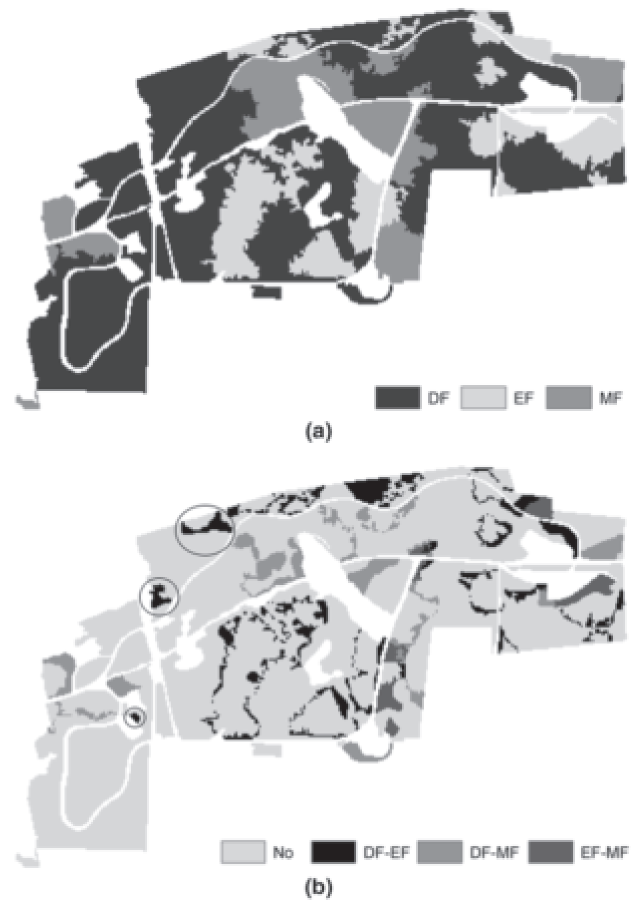

Figure 10. (a) Forest type classification result, and (b) misclassifications on object-specific texture classification using GLCM contrast, correlation, dissimilarity and variance. A color version of this figure is available at the ASPRS website: **www.asprs.org**. (In Figure 10a of the color version, the black line indicates the boundary of individual forest type stands.)

Conclusions

Forest type mapping for a National Park unit was performed using an object-based approach applied to a 4-meter multispectral Ikonos image acquired during the summer. The classification of forest types, including deciduous broadleaf, evergreen coniferous and mixed forests, was achieved through exploration of the effects of combining spectral and contextual texture information. A manually interpreted forest stands geodatabase was employed as a benchmark to investigate the extent to which object-based segmentation and classification can emulate a field-verified manual interpretation of forest types.

Important findings associated with object-based forest type classification on the Ikonos image include:

1. The level of segmentation directly influenced forest type mapping when adopting an object-based approach. In general, classification accuracies were lower for data sets resulting from over- and under-segmentation than optimal segmentation. Overall classification accuracy for GEOBIA results with extreme over-segmentation, i.e., at the scale of 2, was improved by 31 percent (0.42 Kappa) when optimal segmentation (i.e., 19) was used. At the optimal segmentation scale of 19, an overall classification accuracy of 79 percent with a Kappa 0.65 was realized using only with spectral information. Our previous study (Kim *et al.*, 2008) showed the number and average sizes of image objects obtained at segmentation scales of 18 and 19 were comparable to the

number and size of forest stands contained in a manually interpreted and field verified forest type data set.

2. Given the importance of segmentation quality on object-based classification accuracy, an objective method of determining the optimal segmentation level was desired. A series of object-based classification results demonstrated that a spatial autocorrelation analysis, based on Moran's I index values, could discriminate segmentation levels. The analysis yielded lowest, even negative, Moran's I values at optimal segmentations compared with over- and under-segmentations. This analysis is anticipated to reduce processing time and labor of selecting appropriate segmentation scales for object-based forest type mapping with VHR satellite imagery in comparison with a trial-and-error method.
3. Object-specific GLCM texture measures did not produce a notable increase in classification accuracies (ranging from 60 percent to 79 percent for overall accuracy) when they were employed individually with spectral information in classification procedures. However, forest type classification results were enhanced by adopting multiple texture measures. By employing selected multiple texture analysis, classification accuracies were enhanced to 83 percent for overall accuracy with Kappa of 0.71 at the optimal segmentation of scale 19. These improved results were attributed to reducing classification confusion between evergreen and mixed forest types up to 2 percent. An error map, produced from a GEOBIA classified image and manual interpretation, showed that the placement of image objects only differed by 8 percent or less. Some misclassification occurred because of local segmentation quality, and other misclassification occurred at transition areas between two different forest types.
4. It is possible to produce GIS-ready vector polygons of forest type stands from object-based classification of a VHR satellite image for further GIS analysis, thus enhancing the potential for a close coupling between remote sensing and GIS analyses.

Overall, this study resulted in a forest type map that was similar to that of a manual interpretation by adopting object-based image classification with the addition of multiple object-specific GLCM texture measures. The best classification meets accuracy standards that are required for National Park vegetation mapping (over 80 percent in overall accuracy).

With increasing availability of VHR imagery and high demand for mapping natural and cultural resources, the GEOBIA approach offers great potential for automated classification techniques that emulate the delineation and classification of manual interpretation. However, it is important to develop methodologies that estimate optimal segmentations across various landscape units and that enhance the quality of segmentation. In addition, although a single segmentation scale was utilized in this study, future research needs to consider multi-scale segmentation analyses when employing hierarchical classification scheme. That is because a single segmentation scale may not be appropriate for object-based land-use and land-cover classifications.

In future work, we plan to evaluate optimal segmentation quality by using a spatial autocorrelation analysis for other landscapes, e.g., urban or suburban land-use and land-cover, and investigate the relationship between segmentation quality and classification results. Keeping the need for future updating of databases within the National Vegetation Mapping Program in mind, we plan to perform stand-level forest/vegetation GEOBIA classification for a large National Park like Great Smoky Mountains National Park. In addition, we intend to investigate whether it is possible to find a method to assist researchers in identifying the optimal combination of GLCM texture measures for inclusion in GEOBIA classification.

Acknowledgments

The Guilford Courthouse National Military Park vegetation database that was used in this study was created by the Center for Remote Sensing and Mapping Science (CRMS), Department of Geography, the University of Georgia with funding by the National Park Service (NPS) as part of the U.S. Geological Survey and NPS National Vegetation Mapping Program (Cooperative Agreement No. H5028 01 0651). The authors wish to express their appreciation to Teresa Leibfried and Robert Emmott of NPS for their continued support and to the staff of the CRMS for their efforts in creating the vegetation database. The Ikonos imagery used in this study was provided by Space Imaging, Inc. (now GeoEye, Inc.) as a 2005 American Society for Photogrammetry and Remote Sensing (ASPRS) Space Imaging Data Award.

References

Addink, E.A., S.M. de Jong, and E.J. Pebesma, 2007. The importance of scale in object-based mapping of vegetation parameters with hyperspectral imagery, *Photogrammetric Engineering & Remote Sensing*, 72(8):905–912.

Asner, G.P., and A.S. Warner, 2003. Canopy shadow in IKONOS satellite observations of tropical forests and savannas, *Remote Sensing of Environment*, 87:521–533.

Avery, T.E., 1962. *Interpretation of Aerial Photographs*, Second edition, Burgess Publishing Co., 324 p.

Benz, U.C., P. Hofmann, G. Willhauck, I. Lingenfelder, and M. Heynen, 2004. Multi-resolution, object-oriented fuzzy analysis of remote sensing data for GIS-ready information, *ISPRS Journal of Photogrammetry and Remote Sensing*, 58:239–258.

Blaschke, T., 2003. Object-based contextual image classification built on image segmentation, *Proceedings of the 2003 IEEE Workshop on Advances in Techniques for Analysis of Remotely Sensed Data*, 27–28 October, Washington, D.C., pp. 113–119.

Blaschke, T., and J. Strobl, 2001. What's wrong with pixels? Some recent developments interfacing remote sensing and GIS, *GIS-Zeitschrift für Geoinformationssysteme*, 6:12–17.

Brandtberg, T., and T. Warner, 2006. High resolution remote sensing, *Computer Applications in Sustainable Forest Management* (G. Shao and K.M. Reynolds, editors), Springer-Verlag, Dordrecht, Netherlands, pp. 19–41.

Coburn, C.A., and A.C.B. Roberts, 2004. A multiscale texture analysis procedure for improved forest stand classification, *International Journal of Remote Sensing*, 25(2):4287–4308.

Colwell, R.N., 1960. Some uses of infrared aerial photography in the management of wildland areas, *Photogrammetric Engineering*, 26(12):774–785.

Definiens, 2004. *eCognition User Guide 4*, Definiens AG, Germany.

Dorren, L.K.A., B. Maier, and A.C. Seijmonsbergen, 2003. Improved Landsat-based forest mapping in steep mountainous terrain using object-based classification, *Forest Ecology and Management*, 183:31–46.

Ehlers, M., M. Gaehler, and R. Janowsky, 2003. Automated analysis of ultra high resolution remote sensing data for biotope type mapping: New possibilities and challenges, *ISPRS Journal of Photogrammetry and Remote Sensing*, 57:315–326.

Ehlers, M., 2004. Remote sensing for GIS applications: New sensors and analysis methods, *Remote Sensing for Environmental Monitoring, GIS Applications, and Geology III* (M. Ehlers, J.J. Kaufmann, and U. Michel, editors), Proceedings of SPIE, Bellingham, Washington, 5239:1–13.

Federal Geographic Data Committee (FGDC), 2007. *National Vegetation Classification Standard Version 2*, Submitted Draft, 30 November 2006, Edited October 2007, FGDC-STD-005 (Version 2), URL: *http://www.fgdc.gov/standards/projects/FGDC-standards-projects/vegetation/Draft_FGDC_Std_FINAL_Oct2007.doc* (last date accessed: 30 March 2009).

Feitosa, C.U., G.A.O.P. Costa, and T.B. Cazes, 2006. A genetic approach for the automatic adaptation of segmentation parameters, *Commission IV, WG IV/4 on Proceeding of 1st OBIA Conference*, 04–05 July, Salzburg, Austria (International Society for Photogrammetry and Remote Sensing), unpaginated CD-ROM.

Ferro, C.J.S., and T.A. Warner, 2002. Scale and texture in digital image classification, *Photogrammetric Engineering & Remote Sensing*, 68(1):51–63.

Fisher, P., 1997. The pixel: A snare and a delusion, *International Journal of Remote Sensing*, 18(3):679–685.

Franklin, S.E., R.J. Hall, L.M. Moskal, A.J. Maudie, and M.B. Lavigne, 2000. Incorporating texture into classification of forest species composition from airborne multispectral images, *International Journal of Remote Sensing*, 21(1):61–79.

Franklin, S.E., M.A. Wulder, and G.R. Gerylo, 2001a. Texture analysis of Ikonos panchromatic data for Douglas-fir forest age class separability in British Columbia, *International Journal of Remote Sensing*, 22(13):2627–2632.

Franklin, S.E., A.J. Maudie, and M.B. Lavigne, 2001b. Using spatial co-occurrence texture to increase forest structure and species composition classification accuracy, *Photogrammetric Engineering & Remote Sensing*, 67(8):849–855.

Gong, P., D.J. Marceau, and P.J. Howarth, 1992. A comparison of spatial feature extraction algorithms for land-use classification with SPOT HRV data, *Remote Sensing of Environment*, 40:137–151.

Guo, Q., M. Kelly, P. Gong, and D. Liu, 2007. An object-based classification approach in mapping tree mortality using high spatial resolution imagery, *GIScience and Remote Sensing*, 44(1):24–47.

Haralick, R.M., K. Shanmugam, and I. Dinstein, 1973. Textural features for image classification, *IEEE Transactions on Systems, Man and Cybernetics*, SMC, 3(6):610–620.

Haralick, R.M., and K.S. Shanmugam, 1974. Combined spectral and spatial processing of ERTS imagery data, *Remote Sensing of Environment*, 3:3–13.

Hay, G.J., K.O. Niemann, and G.F. McLean, 1996. An object-specific image-texture analysis of H-resolution forest imagery, *Remote Sensing of Environment*, 55:108–122.

Heller, R.C., 1975. *Evaluation of ERTS-1 Data for Forest and Range-land Survey*, USDA Forest Service Research Paper PSW-112, Pacific S.W. Forest and Range Experiment Station, Berkeley, California.

Hiatt, J., 2003. *Guilford Courthouse National Military Park: Cultural Landscape Report*, National Park Service Web, Southeast Regional Office, Cultural Resources Division, URL: *http://www.nps.gov/guco/pphtml/documents.html*, National Park Service, Southeast Regional office, Cultural Resources Division (last date accessed: 30 March 2009).

Hoffer, R.M., and Staff, 1975. *Natural Resource Mapping in Mountainous Terrain by Computer Analysis of ERTS-1 Satellite Data*; Agricultural Experiment Station Research Bulletin 919, Purdue University, West Lafayette, Indiana.

Jensen, J.R., 1979. Computer graphic feature analysis and selection, *Photogrammetric Engineering & Remote Sensing*, 45(11):1507–1512.

Kim, M., and M. Madden, 2006. Determination of optimal scale parameter for alliance-level forest classification of multispectral Ikonos image, *Commission IV, WG IV/4 on Proceeding of 1st OBIA Conference*, 04–05 July, Salzburg, Austria (International Society for Photogrammetry and Remote Sensing), unpaginated CD-ROM.

Kim, M., M. Madden, and T.A. Warner, 2008. Estimation of optimal image object size for the segmentation of forest stands with multispectral Ikonos imagery, *Object-based Image Analysis - Spatial Concepts for Knowledge-driven Remote Sensing Applications* (T. Blaschke, S. Lang, and G.J. Hay, editors), Springer-Verlag, Berlin, pp. 291–307.

Lachowski, H., P. Maus, and N. Roller, 2000. From pixels to decisions: Digital remote sensing technologies for public land managers, *Journal of Forestry*, 98(6):13–15.

Lu, D., and Q. Weng, 2007. Survey of image classification methods and techniques for improving classification performance, *International Journal of Remote Sensing*, 28(5):823–870.

Lund, H.G., W.A. Befort, J.E. Brickell, W.M. Ciesla, E.C. Collins, R.L. Czaplewski, A.A. Disperati, R.W. Douglass, C.W. Dull, J.D. Greer, R.R. Hershey, V.J. LaBau, H. Lachowski, P.A. Murtha, D.J. Nowak, M.A. Roberts, P. Schram, M.D. Shedha, A. Singh, and K.C. Winterberger, 1997. Forestry, *Manual of Photographic Interpretation*: Second edition (W.R. Philipson, editor), American Society for Photogrammetry and Remote Sensing, pp. 399–433.

Madden, M., and T. Jordan, 2004. Database development and analysis for decision makers in National Parks of the Southeast, *Proceedings of ASPRS Fall Conference*, 12–16 September, Kansas City, Missouri (American Society for Photogrammetry and Remote Sensing, Bethesda, Maryland), unpaginated CR-ROM.

Marceau, D.J., P.J. Howarth, J.M.M. Dubois, and D.J. Gratton, 1990. Evaluation of grey-level co-occurrence matrix method for land-cover classification using SPOT imagery, *IEEE Transactions on Geoscience and Remote Sensing*, 28(4):513–519.

Meinel, G., and M. Neubert, 2004. A comparison of segmentation programs for high resolution remote sensing data, *Commission VI in Proceeding of XXth ISPRS Congress*, 12–23 July, Istanbul, Turkey (International Society for Photogrammetry and Remote Sensing), unpaginated CD-ROM.

Metzler, J.W., and S.A. Sader, 2005. Model development and comparison to predict softwood and hardwood per cent cover using high and medium spatial resolution imagery, *International Journal of Remote Sensing*, 26(17):3749–3761.

National Park Service (NPS), 2008. Vegetation Mapping Program, U.S. Geological Survey (USGS) Biological Resources Discipline (BRD) and National Park Service, URL: *http://science.nature.nps.gov/im/inventory/veg/index.cfm* (last date accessed: 30 March 2009).

NatureServe, 2007. *Accuracy Assessment: Guilford Courthouse National Military Park*, Final Report to the National Park Service, Durham, North Carolina, 5 p.

Read, J.M., D.B. Clark, E.M. Venticinque, and M.P. Moreira, 2003. Application of merged 1-m and 4-m resolution satellite data to research and management in tropical forest, *Journal of Applied Ecology*, 40:592–600.

Ryherd, S., and C. Woodcock, 1996. Combining spectral and texture data in the segmentation of remotely sensed images, *Photogrammetric Engineering & Remote Sensing*, 62(2):181–194.

Shiewe, J., L. Tufte, and E. Ehlers, 2001. Potential and problems of multi-scale segmentation methods in remote sensing, *GIS-Zeitschrift für Geoinformationssysteme*, 6:34–39.

Souza, C.M., and D. Roberts, 2005. Mapping forest degradation in the Amazon region with IKONOS images, *International Journal of Remote Sensing*, 26(3):425–429.

Teng, W.T., E.R. Loew, D.I. Ross, V.G. Zsilinsky, C.P. Lo, W.R. Philipson, W.D. Philpot, and S.A. Morain, 1997. Fundamentals of photographic interpretation, *Manual of Photographic Iinterpretation* (W.R. Philipson, editor), American Society for Photogrammetry and Remote Sensing, pp. 49–110.

Townshend, J.R.G, C. Huang, S.N.V. Kalluri, R.S. Defries, S. Liang, and K. Yang, 2000. Beware of per-pixel characterization of land-cover, *International Journal of Remote Sensing*, 21(4):839–843.

Wang, L., W.P. Sousa, and P. Gong, 2004a. Integration of object-based and pixel-based classification for mapping mangroves with Ikonos imagery, *International Journal of Remote Sensing*, 25(24):5655–5668.

Wang, L., W.P. Sousa, P. Gong, and G.S. Biging, 2004b. Comparison of IKONOS and QuickBird images for mapping mangrove species on the Caribbean coast of Panama, *Remote Sensing of Environment*, 91(3–4):432–440.

Welch, R., M. Remillard, and R. Doren, 1995. GIS database development for South Florida's National Parks and Preserves, *Photogrammetric Engineering & Remote Sensing*, 61(11):1371–1381.

Welch, R., M. Madden, and R. Doren, 1999. Mapping the Everglades, *Photogrammetric Engineering & Remote Sensing*, 65(2):163–170.

Welch, R., M. Madden, and T. Jordan, 2002. Photogrammetric and GIS techniques for the development of vegetation databases of mountainous areas: Great Smoky Mountains National Park, *ISPRS Journal of Photogrammetry and Remote Sensing*, 57:53–68.

Woodcock, C.E., and A.H. Strahler, 1987. The factor of scale in remote sensing, *Remote Sensing of Environment*, 25:349–379.

Wulder, M.A., J.C. White, K.O. Niemann, and T. Nelson, 2004. Comparison of airborne and satellite high spatial resolution data for the identification of individual trees with local maxima filtering, *International Journal of Remote Sensing*, 25(11):2225–2232.

Yu, Q., P. Gong, N. Clinton, G. Biging, M. Kelly, and D. Shirokauer, 2006. Object-based detailed vegetation classification with airborne high spatial resolution remote sensing imagery, *Photogrammetric Engineering & Remote Sensing*, 72(7):799–811.

Zhang, Y., 1999. Optimization of building detection in satellite images by combining multispectral classification and texture filtering, *International Journal of Remote Sensing*, 54:50–60.

Zhang, C., S.E. Franklin, and M.A. Wulder, 2004. Geostatistical and texture analysis of airborne-acquired images used in forest classification, *International Journal of Remote Sensing*, 25(4):859–865.